Faraday Discussions

Accepted Manuscript

This manuscript will be presented and discussed at a forthcoming Faraday Discussion meeting. All delegates can contribute to the discussion which will be included in the final volume.

Register now to attend! Full details of all upcoming meetings: http://rsc.li/fd-upcoming-meetings

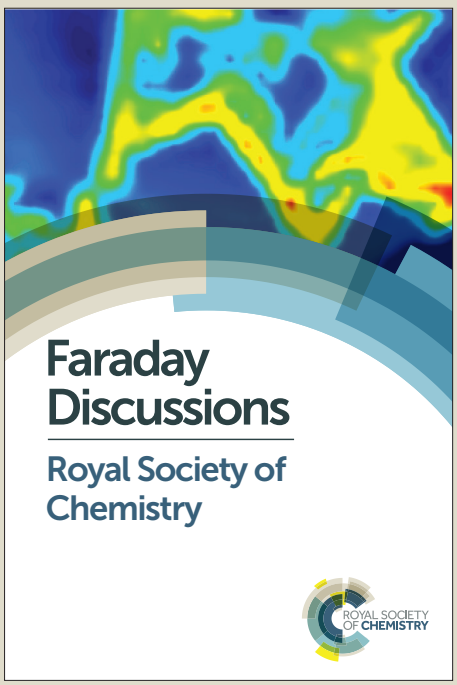

This is an *Accepted Manuscript*, which has been through the Royal Society of Chemistry peer review process and has been accepted for publication.

Accepted Manuscripts are published online shortly after acceptance, before technical editing, formatting and proof reading. Using this free service, authors can make their results available to the community, in citable form, before we publish the edited article. We will replace this *Accepted Manuscript* with the edited and formatted *Advance Article* as soon as it is available.

You can find more information about *Accepted Manuscripts* in the Information for Authors.

Please note that technical editing may introduce minor changes to the text and/or graphics, which may alter content. The journal's standard Terms & Conditions and the Ethical guidelines still apply. In no event shall the Royal Society of Chemistry be held responsible for any errors or omissions in this *Accepted Manuscript* or any consequences arising from the use of any information it contains.

ROYAL SOCIETY OF CHEMISTRY

www.rsc.org/faraday_d

Active site densities, oxygen activation and adsorbed reactive oxygen in alcohol activation on npAu catalysts

Lu-Cun Wang[a] , C. M. Friend[a,b] and Robert J. Madix [b]

[a] Department of Chemistry and Chemical Biology, Harvard University, Cambridge, MA, 02138, USA
[b] School of Engineering and Applied Sciences, Harvard University, Cambridge, MA, 02138, USA.
E-mail: rmadix@seas.harvard.edu; Fax: +617 496 9489; Tel: +617 496 9489

Abstract

The activation of molecular O_2 as well as the reactivity of adsorbed oxygen species is of central importance in aerobic selective oxidation chemistry on Au-based catalysts. Herein, we address the issue of O_2 activation on the unsupported nanoporous gold (npAu) catalysts by applying a transient pressure technique, temporal analysis of products (TAP) reactor, to measure the saturation coverage of atomic oxygen, its collisional dissociation probability, the activation barrier for O_2 dissociation, and the facility with which adsorbed O species activates methanol, the initial step in the catalytic cycle of esterification. The results from these experiments indicate that molecular O_2 dissociation is associated with surface silver, that the density of reactive sites is quite low, that adsorbed oxygen atoms do not spill over from the sites of activation onto the surrounding surface, and that methanol reacts quite facilely with the adsorbed oxygen atoms. In addition, the O species from O_2 dissociation exhibits reactivity for selective oxidation of methanol but not for CO. The TAP experiments also revealed that the surface of npAu catalyst is saturated with adsorbed O under steady state reaction conditions, at least for the pulse reaction.

1.Introduction

Metallic gold is used as exceptional catalyst for a wide range of reactions, in particular the oxygen-assisted chemical transformations, such as CO oxidation and esterification of alcohols.[1-3] Gold nanoparticles dispersed on reducible oxides are the most commonly used gold catalysts for various catalytic applications.[1,4] This type of catalysts, however, is susceptible to deactivation resulting from the growth of gold particle size under working conditions.[4] Recently, a new type of unsupported, nanoporous gold (npAu) catalysts with ligament sizes between 20 – 100 nm has been demonstrated to be highly efficient for these key oxidation processes.[3,5-10] In addition to its excellent activity, the npAu material is also highly selective for ester formation.[3,7,8,10] More importantly, these materials are very robust, showing negligible losses of activity or selectivity for even months under reaction conditions.[8]

It is well established that on model gold surfaces the adsorbed *atomic* oxygen, usually formed via ozone decomposition[11] or electron-induced dissociation of NO_2[12], directly activates and drives the catalytic cycles of alcohol coupling reactions.[3,7,8,10,13] Since molecular O_2 is used under practical catalytic conditions, understanding the mechanism of O_2 activation processes on the surfaces of 'real-world' gold catalysts is critical to develop new materials with improved catalytic performances.

Molecular O_2 is readily dissociated on npAu materials even at low temperature; the nature and density of reactive centers for this process, however, still remains elusive. The npAu employed in the catalytic studies contains a small amount of Ag (1-3%) that results from its synthesis from an Ag/Au bulk alloy.[3,5,6] Taking into account the fact that O_2 can readily dissociate on Ag surfaces, Ag(110) surface in particular,[14] it is reasonable to speculate that the residual Ag is involved in the dissociation of molecular O_2 on npAu catalysts, as proposed on the basis of numerous experimental and theoretical studies.[15-19] On the other hand, low-coordinated Au sites, such as edge, step, or kink sites, have also been suggested to be responsible for O_2 activation and catalytic activity.[6,20,21] This viewpoint is suggested by transmission electron microscopy (TEM) studies[22] that reveal a high incidence of step and kink sites on the material. However, recent studies with extremely pure npAu synthesized from an intermetallic AuZr alloy (bulk residual Zr content ~0.03%) exhibit very low activity toward CO oxidation,[23] which indicates that Ag impurities play a key role in the dissociation of O_2 on npAu.

As a transient reaction technique, the temporal analysis of products (TAP) reactor has been successfully applied in numerous studies on the mechanism and dynamics of adsorption and reaction processes on catalyst surfaces.[24] The high detection sensitivity and time resolution renders this technique an ideal tool to study the dynamic and kinetic behaviors of catalytic reaction as well as to investigate the nature and reactivity of intermediate species, such as adsorbed oxygen, in both qualitative and quantitative ways.

In this work, using a TAP reactor, we address the issue of O_2 activation on npAu catalysts by measuring the saturation coverage of atomic oxygen on npAu, its surface-averaged initial collisional dissociation probability, the activation barrier for O_2 dissociation, and the facility with which adsorbed O species activates methanol, the initial step in the catalytic cycle of esterification. The results from these TAP experiments support the hypothesis that molecular oxygen dissociation is associated with surface silver, that the density of reactive sites is quite low, that adsorbed oxygen atoms do not spill over from the sites of activation onto the surrounding surface, and that methanol reacts quite facilely with the adsorbed oxygen atoms.

2. Experimental

2.1 Synthesis of hollow npAu microspheres

Hollow npAu microspheres were synthesized according to a previously reported method.[8] Briefly, 10 μm cross-linked polystyrene-divinylbenzene (PS-DVB) microspheres were coated with Ag and Au in a ratio of 85:15 via electroless deposition in aqueous solution. The AgAu-coated microspheres were subsequently calcined at 450 °C for one hour in air (39 mL/min) in a flow reactor to alloy the metals and to remove the PS-DVB core and any residual organic stabilizing agents from the synthesis procedure. The annealed hollow AgAu microspheres were dealloyed in concentrated nitric acid until the Ag composition was 1%. The BET surface area was determined to be 2 m^2 g^{-1} after activation (see below for the detailed procedure).

2.2 TAP experiments

The pulse experiments were carried out in a commercial TAP-2 reactor (Fig. 1).[24] In a typical pulse response experiment a narrow pulse of reactant gas (ca. 10^{-8} mol/pulse, pulse width 0.135 ms) was injected into a packed-bed microreactor using a high-speed,

magnetically controlled pulse valve. The microreactor was a quartz tubular reactor with a length of 38 mm and a diameter of 6.35 mm, housing an internal thermocouple. The microreactor sat on top of a high-throughput vacuum chamber (10^{-8} to 10^{-9} Torr) containing a RGA200 mass spectrometer, which was used to detect the effluent from the reactor. The npAu catalyst was sandwiched in a thin-zone configuration in the middle of the microreactor packed among inert quartz particles with diameters between 250 and 300 μm. Pulse sizes were chosen to ensure Knudsen flow throughout the reactor.

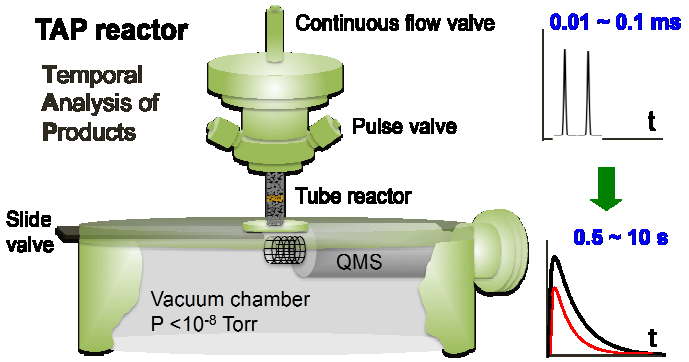

Fig. 1 Scheme of the TAP-2 reactor

The diffusion–reaction processes in the TAP pulse experiment, taking O_2 dissociation on npAu catalyst for example, can be described using a model based on the following partial differential equation[24]:

$$\varepsilon_b \frac{\partial C_{O_2}}{\partial t} = D_{k,eff} \frac{\partial^2 C_{O_2}}{\partial x^2} - kC_{z,total} C_{O_2} f(\theta_O) \quad (1)$$

where f(θ) is an unspecified coverage dependence of the dissociation probability of O_2. The initial condition is

$$0 \le x \le L, \quad t = 0, \quad C_{O_2} = \delta_z \frac{N_{O_2}}{\varepsilon_b A} \quad (2)$$

and boundary conditions are

$$x = 0, \quad \frac{\partial C_{O_2}}{\partial z} = 0 \quad (3)$$

$$x = L, \quad C_{O_2} = 0 \quad (4)$$

In the case of very low reaction probability, the diffusion–reaction processes can be approximated as the diffusion-only case (Fig. 2):

$$\varepsilon_b \frac{\partial C_{O_2}}{\partial t} = D_{k,eff} \frac{\partial^2 C_{O_2}}{\partial x^2} \quad (5)$$

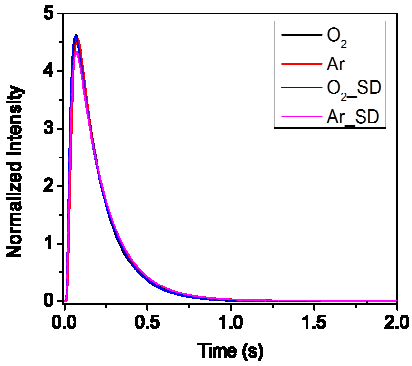

Fig. 2 Experimental and simulated standard diffusion (SD) pulse response curves of O_2 and Ar on npAu catalyst at 423 K.

For standard diffusional response curve, the dimensionless peak position τ_p is a constant,[24] namely,

$$\tau_p = \frac{t_p D_e}{\varepsilon L^2} = \frac{1}{6} \quad (6)$$

where t_p is the maximum of the experimentally derived response curves (0.077 s), D_e the effective Knudsen diffusivity of the gas in the packed bed (26.2 cm^2 s^{-1}), ε the fractional voidage (0.84) of the packed bed, L the length of the reactor (3.8 cm). Accordingly, the Knudsen diffusion characteristic of the species throughout the reactor, such as methanol and O_2, can be directly determined from the corresponding experimental pulse responses (Fig. 2). The reaction rate constants in Eqn. (1) can be determined either by solving the equation numerically or from moment analysis with presumed reaction kinetics.[24]

Prior to all the TAP experiments, the pulse size was calibrated by using argon gas. To do this, a calibrated volume (***V***) filled with Ar at a given pressure was connected to the pulse valve. The pressure drop (***ΔP***) after a certain number of pulses (***n***) was used to calculate the average pulse size (number of molecules per pulse, ***N***) as follows

$$N = \frac{\Delta P \cdot V}{R \cdot T \cdot n} \quad (7)$$

The detection sensitivity factor, ***λ,*** for Ar could be then determined from the measured pulse intensity (***I***, the integrated area under the pulse curve of mass 40) and the corresponding pulse size (***N***, the number of molecules in each pulse) as follows:

$$\lambda = \frac{N}{I} \quad (8)$$

The detection sensitivity factors for reactant and products including methanol, O_2, and CO_2 were determined by pulsing a mixture with Ar with known composition. With a mixture of O_2/Ar (ratio η), the sensitivity factor for O_2 (λ_{O2}), can be determined by,

$$\lambda_{O_2} = \frac{N_{O_2}}{I_{O_2}} = \frac{\eta \cdot N_{Ar}}{I_{O_2}} = \frac{\eta \cdot \lambda_{Ar} \cdot I_{Ar}}{I_{O_2}} \quad (9)$$

The amount of stable adsorbed active oxygen formed on the npAu catalyst by O_2 dissociation was determined by titration with a sequence of methanol pulses. Prior to the pulse experiments, the catalyst was activated by ozone treatment via a leak valve (10^{-6}

Torr for 1 min) at 423 K and completely reduced with CH_3OH/Ar pulses. Note that under pulse reaction conditions in the TAP reactor formaldehyde was detected as the predominant product (selectivity >98%) in the reaction of methanol with adsorbed oxygen. The O_2 uptake was quantified either from the total amount of formaldehyde formation (m/z=30, parent ion) from calibrated methanol pulses or directly from the O_2 uptake during O_2 exposure (see Fig. 3). The packing material was determined to be inert in these experiments under identical conditions.

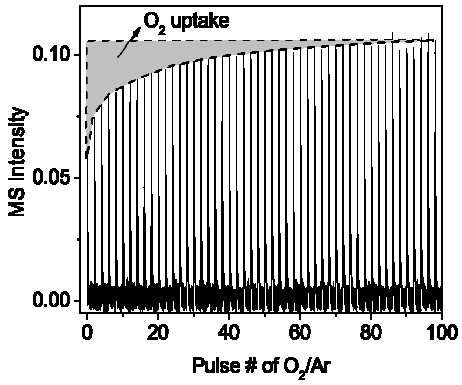

Fig. 3 Sequence of multiple O_2/Ar pulses (pulse separation = 2 s) dosed on activated npAu at 423 K. The grey area indicates the total O_2 uptake during the pulsing.

Since the m/z=30 fragment is not unique to formaldehyde, the overlapping contributions from cracking of methanol were subtracted according to the relative ion yields obtained in a blank experiment with methanol pulsing over the inert packing materials, i.e., SiO_2. After subtracting the fragment contributions from methanol, the mass intensity was then converted into the number of formaldehyde molecules from each pulse by using the detection sensitivity factor of methanol relative to Ar, assuming that these molecules have comparable mass spectrometer detection factors, which proves to be the case for CO_2 and Ar. No formaldehyde was produced upon exposure to methanol pulses on the pristine sample, i.e. without prior exposure to O_2.

3. Results and Discussion

3.1 Capacity of npAu catalyst in O_2 dissociation

We first examined the activation of O_2 on the npAu catalyst by exposing the catalyst at 423 K sequentially to 100 O_2 pulses and 100 CH_3OH/Ar pulses. The oxygen uptake from O_2 exposure, determined either by the O_2 response pulse exiting the reactor or by the total amount of formaldehyde formed during subsequent methanol titration, increases rapidly as the O_2 dosage increases and then approaches saturation (Fig. 4a).

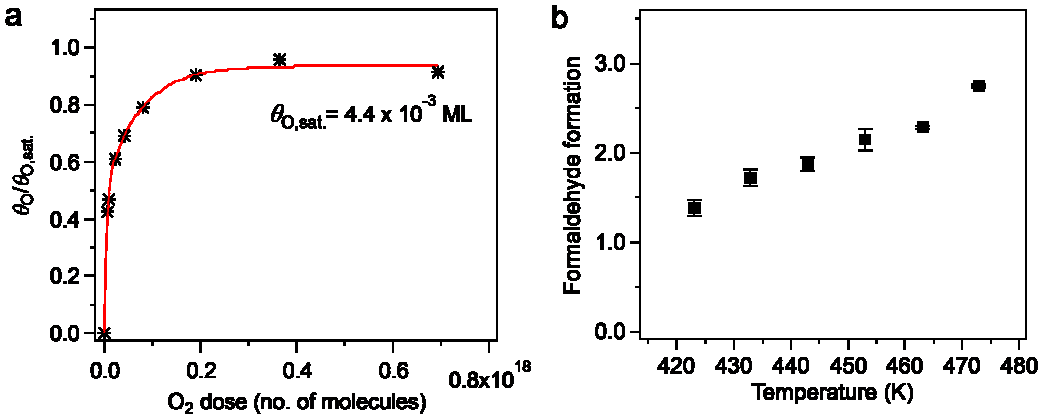

Fig. 4 a) The fractional coverage of adsorbed oxygen atoms on the npAu catalyst versus O_2 dose from sequential pulses of O_2 at 423 K. b) Formaldehyde formation during titration of active oxygen from O_2 dissociation on the npAu catalyst at different temperatures (single pulse of O_2 followed by titration with 100 pulses of CH_3OH/Ar).

Based on the amount of npAu (27 mg), the BET surface area (2 m^2 g^{-1}) after activation, and the amount of formaldehyde formed at the saturation point (3.1×10^{15} molecules), the surface concentration of adsorbed O at saturation coverage resulting from the O_2 pulsing was calculated to be 6.2×10^{16} O atoms m^{-2} or 4.4×10^{-3} ML, assuming a surface atomic density of 1.4×10^{19} atoms m^{-2} for the Au(111) surface. It is possible that O could spill over onto the surface (the saturation density on gold being near 1.0 M)[25] but this apparently does not occur at these temperatures.

From points in the initial linear portion of the uptake vs. exposure curve (Fig. 4a) the initial dissociative sticking probability of O_2 at the lowest initial oxygen coverage on the activated npAu catalyst at 423 K was computed to be ~1×10^{-7} at 423 K. This value is significantly lower than that on single-crystal Ag surfaces[26,27] and on Ag powder[28] or even on supported Ag catalysts[29].

By methanol titration following O_2 exposure at different temperatures (473 K to 423 K), the apparent activation energy (E_a) for O_2 dissociation on the npAu catalyst was determined to be 5.0 ± 0.4 kcal/mol (Fig. 4b). This result is comparable to that reported on Ag single-crystal surfaces[27] but significantly below that estimated for single-crystal Au surfaces[25,30,31]. Experimentally, neither stepped single crystals nor polycrystalline Au surfaces dissociate molecular oxygen even at high temperature or high-pressure conditions.[14,25,31]

3.2 Stability of O_a from O_2 dissociation

By varying the delay time between O_2 and subsequent methanol pulse, we further investigated the stability of the active oxygen species formed from O_2 dissociation on the npAu catalyst. The results showed that the amount of formaldehyde formation decreases rapidly with the delay time below 0.5 s and then kept almost constant as the delay time was further extended up to 2 s (Fig. 5). The higher formaldehyde formation when the delay time is below 0.5 s may be explained by the enhanced total O_2 uptake due to the overlap between O_2 and methanol pulses (see Fig. 2). Since methanol can readily react with adsorbed O, it is reasonable to deduce that in the presence of excess methanol, the active sites (adsorbed O) can be rapidly regenerated, resulting in higher total O_2 uptake at

shorter delay time. With extended delay time between O_2 and methanol pulses, more O_2 will leave the catalyst bed before the methanol pulse arrives at the catalyst surface, leading to less O_2 dissociation and thus decreasing formaldehyde formation.

Note that adsorbed atomic O is quite stable on both Ag and Au single crystal surfaces, desorbing by atom recombination near 550 K.[14,27,30] It is possible, however, that with increased time between pulses the adsorbed O could change reactivity by conversion to another binding state. Since there was little variation in the amount of various products at a delay time longer than 0.5 s (Fig. 5), it appears that the active oxygen species from O_2 dissociation on the npAu surface at 423 K does not undergo a transformation into another form with different reactivity.

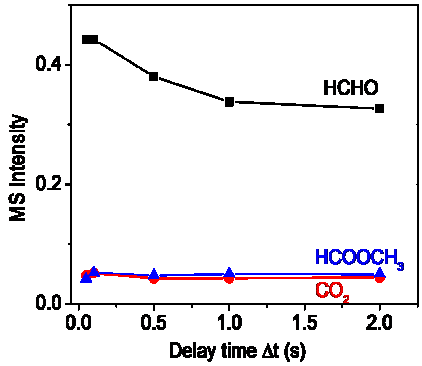

Fig. 5 The formation of various products including formaldehyde, methyl formate, and CO_2 as a function of delay time between 1 pulse of CH_3OH/Ar and 1 pulse of O_2.

3.3 Reactivity of active adsorbed O with CO and methanol

To determine the reactivity of CO and methanol with the active adsorbed oxygen species, sequential pulsing of O_2 and CO/CH_3OH was conducted. Following an initial 100 pulses of O_2, the introduction of CO pulses resulted in the formation of only a very small amount of CO_2 at the beginning of the pulse cycle (Fig. 6a), but there was no measurable consumption of CO in parallel with the CO_2 formation. In addition, negligible O_2 uptake was detected if O_2 was re-introduced after CO pulsing (Fig. 6b). These results clearly indicate that the CO_2 formation was not from the reaction of CO with the active adsorbed oxygen. We attribute the CO_2 to displacement from other regions of the reactor. When methanol is introduced after the CO pulses, however, initially almost all the methanol is converted with concomitant formation of formaldehyde, and the reaction abates after approximately 100 methanol pulses (Fig. 6a).

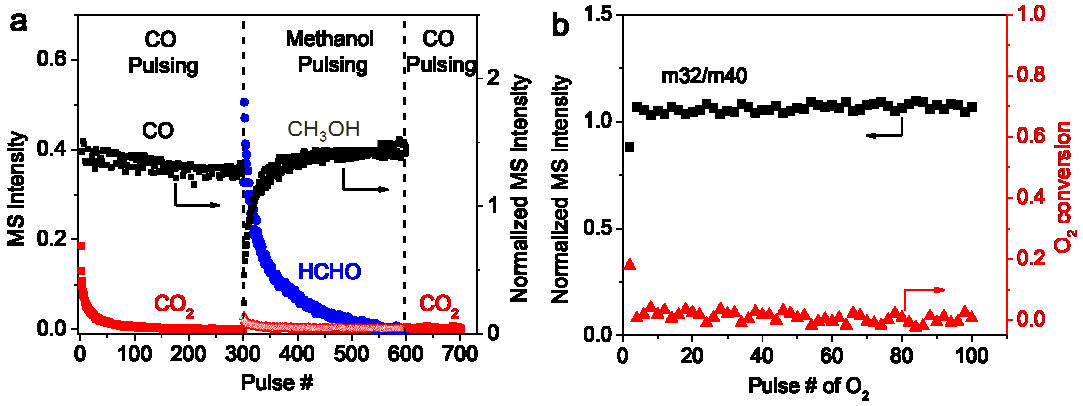

Fig. 6 a) Sequential pulsing of CO and methanol over npAu after 100 pulses of O_2. b) Normalized O_2 pulse intensity and the corresponding O_2 conversion in each pulse during O_2 pulsing after exposure to CO pulses.

It is clear that methanol can be catalytically activated on the npAu catalyst when pulsed simultaneously with O_2 (see Fig. 7a), producing formaldehyde as the predominant product under pulse conditions. Surprisingly, when O_2 pulses were interrupted at the steady state there was still notable amount of formaldehyde formation, which, nevertheless, underwent an exponential decay with continuous methanol pulses. This observation indicates that there is a certain amount of oxygen species (~3×10^{-3} ML) on the catalyst surface under steady-state methanol oxidation reaction in the TAP reactor, which might be also the case for the reaction in the flow reactor under steady state conditions.

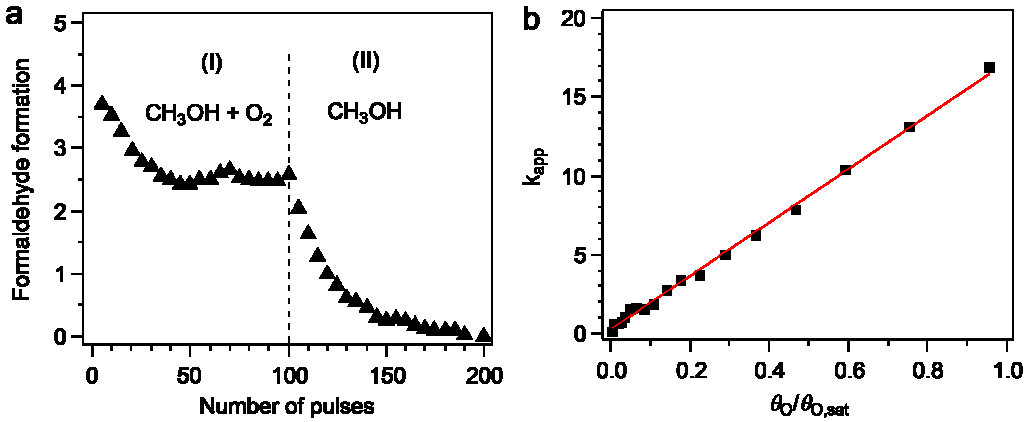

Fig. 7 a) Formaldehyde formation during pulse reaction of methanol with O_2 on activated npAu catalyst at 423 K. b) Apparent rate constant as a function of the fractional O coverage during titration after simultaneous pulsing of O_2 and CH_3OH at 423 K.

Assuming first-order kinetics for reaction of methanol with adsorbed O (second stage in Fig. 7a), the apparent kinetic constant k_{app} can be calculated by the following expression[32,33]

$$k_{app} = \frac{X}{1-X}\frac{1}{\tau_{residence}} \qquad (10)$$

$$\tau_{res} = \varepsilon(\frac{L_{cat}L_{in2}}{D}) \quad (71)$$

where X is the conversion of methanol in each pulse, τ_{res} (s) is the mean residence time of methanol gas in the catalytic zone and is the same for each pulse, L_{cat} is the length of the catalyst zone, L_{in2} is the length of the second inert zone, and D is the diffusivity in the catalyst zone.

On the other hand, k_{app} can be related to surface coverage and the intrinsic constant by

$$k_{app} = \frac{m_{cat}}{V_G} C_{Z,total} k\theta_O \quad (12)$$

where m_{cat} (g) is the catalyst mass, V_G (m^3) the void volume in the catalyst zone, $C_{Z,\,total}$ the total active sites for O_2 dissociation, k (m^3 mol^{-1} s^{-1}) the intrinsic rate constant, θ_O the fractional coverage of adsorbed oxygen.

Based on the data shown in Fig. 7a, $C_{Z,total}$ can be determined from the total amount of formaldehyde formation, X and θ_O for each pulse of methanol can be calculated from the formaldehyde formation and the corresponding methanol dose in each pulse. τ_{res} is calculated to be 0.006078 s. The k_{app} derived from Eqn. (10) is then plotted as a function of θ_O (see Fig. 7b) and the slope is determined to be 17 s^{-1}. Combining the m_{cat} (27 mg), V_G (0.041 cm^3), and $C_{Z,\,total}$ (1.564×10^{-7} mol g_{cat}^{-1}), the intrinsic rate constant k was calculated to be 165 m^3 mol^{-1} s^{-1}, from which, in turn, yields a reaction probability of ~1.3×10^{-8} of methanol with an active surface O atom. It is notable that this reaction probability is nearly an order of magnitude smaller than that for activation of O_2 on the bare surface (~10^{-7}), leading to the conclusion that the active sites should be nearly saturated with O in the steady state. In fact, the quantification result indeed showed that the total amount of the remnant adsorbed O species at the steady-state pulse reaction, i.e., after 100 simultaneous pulses of methanol and O_2 (Fig. 7a), is close to the saturation coverage of O as determined above (see Fig. 4a).

4. Conclusions

In this work, we have determined the saturation coverage of atomic oxygen on np(Ag)Au microspheres (~4×10^{-3} ML), the initial collisional dissociation probability of O_2 with the npAu surface (~1×10^{-7}), and the apparent activation energy of O_2 dissociation on npAu catalyst (5.0 kcal/mol). These results suggest that the active site density for O_2 dissociation on the npAu catalyst is very low and that some form of AgAu bimetallic site is responsible for O_2 activation. The oxygen species formed by exposure to O_2 pulses under TAP conditions is only active for methanol and gives partial oxidation products. The kinetic study of O_2 activation suggests that the surface of npAu catalyst is saturated with adsorbed O under steady state reaction conditions, at least for pulse reaction in the TAP reactor.

Acknowledgements

This work was supported as part of the Integrated Mesoscale Architectures for Sustainable Catalysis, an Energy Frontier Research Center funded by the U.S. Department of Energy, Office of Science, Basic Energy Sciences under Award # DE-SC0012573.

Notes and references

1. M. Haruta, T. Kobayashi, H. Sano, and N. Yamada, *Chem. Lett.*, 1987, **16**, 405–408.
2. E. Taarning, K. Egeblad, R. Madsen, and C. H. Christensen, *Catal Lett*, 2007.
3. A. Wittstock, V. Zielasek, J. Biener, C. M. Friend, and M. Bäumer, *Science*, 2010, **327**, 319–322.
4. G. C. Bond and D. T. Thompson, *Catal. Rev. Sci. Eng.*, 1999, **41**, 319–388.
5. V. Zielasek, B. Jürgens, C. Schulz, J. Biener, M. M. Biener, A. V. Hamza, and M. Bäumer, *Angew. Chem. Int. Ed.*, 2006, **45**, 8241–8244.
6. C. Xu, J. Su, X. Xu, P. Liu, H. Zhao, F. Tian, and Y. Ding, *J. Am. Chem. Soc.*, 2007, **129**, 42–43.
7. K. M. Kosuda, A. Wittstock, C. M. Friend, and M. Bäumer, *Angew. Chem. Int. Ed.*, 2012, **51**, 1698–1701.
8. M. L. Personick, B. Zugic, M. M. Biener, J. Biener, R. J. Madix, and C. M. Friend, *ACS Catal.*, 2015, **5**, 4237–4241.
9. L.C. Wang, K. J. Stowers, B. Zugic, M. M. Biener, J. Biener, C. M. Friend, and R. J. Madix, *Catal. Sci. Technol.*, 2015, **5**, 1299–1306.
10. L.C. Wang, K. J. Stowers, B. Zugic, M. L. Personick, M. M. Biener, J. Biener, C. M. Friend, and R. J. Madix, *J. Catal.*, 2015, **329**, 78–86.
11. B. K. Min, A. R. Alemozafar, D. Pinnaduwage, X. Deng, and C. M. Friend, *J. Phys. Chem. B*, 2006, **110**, 19833–19838.
12. B. K. Min, X. Deng, D. Pinnaduwage, R. Schalek, and C. M. Friend, *Phys. Rev. B*, 2005, **72**, 121410.
13. B. Xu, R. J. Madix, and C. M. Friend, *Acc. Chem. Res.*, 2014, **47**, 761–772.
14. A. G. Sault, R. J. Madix, and C. T. Campbell, *Surf. Sci.*, 1986, **169**, 347–356.
15. A. Wittstock, B. Neumann, A. Schaefer, K. Dumbuya, C. Kübel, M. M. Biener, V. Zielasek, H.-P. Steinrück, J. M. Gottfried, J. Biener, A. Hamza, and M. Bäumer, *J. Phys. Chem. C*, 2009, **113**, 5593–5600.
16. J. L. C. Fajín, M. N. D. S. Cordeiro, and J. R. B. Gomes, *Chem. Commun.*, 2011, **47**, 8403–8405.
17. L. V. Moskaleva, S. Röhe, A. Wittstock, V. Zielasek, T. Klüner, K. M. Neyman, and M. Bäumer, *Phys. Chem. Chem. Phys.*, 2011, **13**, 4529–4539.
18. L. C. Wang, Y. Zhong, D. Widmann, J. Weissmüller, and R. J. Behm, *ChemCatChem*, 2012, **4**, 251–259.
19. L. C. Wang, Y. Zhong, H. Jin, D. Widmann, J. Weissmüller, and R. J. Behm, *Beilstein J. Nanotechnol.*, 2013, **4**, 111–128.
20. C. Xu, X. Xu, J. Su, and Y. Ding, *J. Catal.*, 2007, **252**, 243–248.
21. N. Lopez, T. Janssens, B. S. Clausen, Y. Xu, M. Mavrikakis, T. Bligaard, and J. K. Nørskov, *J. Catal.*, 2004, **223**, 232–235.
22. T. Fujita, P. Guan, K. McKenna, X. Lang, A. Hirata, L. Zhang, T. Tokunaga, S. Arai, Y. Yamamoto, N. Tanaka, Y. Ishikawa, N. Asao, Y. Yamamoto, J. Erlebacher, and M. Chen, *Nat. Mater.*, 2012, **11**, 775–780.
23. T. Déronzier, F. Morfin, L. Massin, M. Lomello, and J.-L. Rousset, *Chem. Mater.*, 2011, **23**, 5287–5289.
24. J. T. Gleaves, G. S. Yablonskii, and P. Phanawadee, *Appl. Catal. A: Gen.*, 1997, **160**, 55–88.

25. J. Kim, E. Samano, and B. E. Koel, *Surf. Sci.*, 2006, **600**, 4622–4632.
26. M. Bowker, M. A. Barteau, and R. J. Madix, *Surf. Sci.*, 1980, **92**, 528–548.
27. C. T. Campbell, *Surf. Sci.*, 1985, **157**, 43–60.
28. M. Bowker, P. Pudney, and G. Roberts, *J. Chem. Soc., Faraday Trans.*, 1989, **85**, 2635–2640.
29. M. Dean and M. Bowker, *Appl. Surf. Sci.*, 1988, **35**, 27–40.
30. J. M. Gottfried, K. J. Schmidt, and S. Schroeder, *Surf. Sci.*, 2003, **525**, 184–196.
31. P. Legare, L. Hilaire, M. Sotto, and G. Maire, *Surf. Sci.*, 1980, **91**, 175–186.
32. E. A. Redekop, G. S. Yablonsky, D. Constales, P. A. Ramachandran, C. Pherigo, and J. T. Gleaves, *Chem. Eng. Sci.*, 2011, **66**, 6441–6452.
33. G. S. Yablonsky, M. Olea, and G. B. Marin, *J. Catal.*, 2003, **216**, 120-134.